

SHORT
COMMUNICATIONS

Fe/Cr and Cu/Cr Film Pressure-Sensitive Elements

I. M. Pазukha and I. E. Protsenko

Sumy State University, ul. Rimskogo-Korsakova 2, Sumy, 40007 Ukraine

e-mail: protsenko@aph.sumdu.edu.ua

Received June 30, 2009

Abstract—A pressure-sensitive element based on Fe/Cr or Cu/Cr film composition is described. The role of interdiffusion and phase formation is discussed, and the interface stability is studied.

DOI: 10.1134/S1063784210040249

INTRODUCTION

The thermoresistive, tensoresistive, magneto-resistive, optical, etc., properties of thin films remain an object of intense research, since they are viewed as candidate materials for sensitive elements in different sensors [1–7]. Here, the point in question is the feasibility of thin-film tensoresistors [4, 8].

Tensoresistors are applied not only in strain gauges, they can also be used as sensitive elements of pressure sensors, which are finding application in measuring the pressure in fluids; under high humidity conditions; in the presence of vibration, impacts, overloading; etc. [7, 9–11]. For example, the developmental prototype of a pressure sensor based on In and Sn films was suggested in [7]. This sensor has piezoresistive coefficient $k = -4.3 \times 10^{-11} \text{ Pa}^{-1}$, which corresponds to gauge factor $\gamma = -2.8$ and allows one to measure the pressure in the range $(-6...+6) \times 10^4 \text{ Pa}$.

In [11], a manganine-based sensitive element for a pressure sensor was suggested that offers a high piezoresistive coefficient ($k = 17.3 \text{ MPa}^{-1}$) and can measure a considerable pressure drop.

If a film system is used as the sensitive element of a sensor, the operating stability of the sensor will be to a great extent determined by processes at interfaces. Therefore, we conducted a series of experiments aimed at studying the processes of phase formation and atomic interdiffusion, which influence the interface stability, with the aim of creating a pressure-sensitive element with stable operating characteristics.

EXPERIMENTAL

Figure 1 shows the setup used to study the physics of a pressure sensor, the operating part of which is thin ($d = 0.5 \text{ mm}$) PTFE membrane 1. Copper contact pads 3 with adhesion-improving chromium sublayer 4 are applied on the surface of the membrane, which is then covered by pressure-sensitive element 2 in the form of a single-layer or multilayer film. To the contact pads, silver push contacts are attached. Rubber seals 5

provide good fixation of the push contacts on the surfaces of the contact pads.

The sensitive element was applied on the membrane and contact pads by thermal evaporation (Cu and Cr layers) and electron-beam evaporation (Fe) in a VUP-5M vacuum chamber (a residual gas pressure of $\sim 10^{-4} \text{ Pa}$) with rates $\omega = 2.0\text{--}2.5 \text{ (Cu)}$, $0.2\text{--}0.8 \text{ (Cr)}$, and $2\text{--}3 \text{ (Fe)} \text{ nm/s}$. The substrate temperature was kept at 300 K (it was measured using a

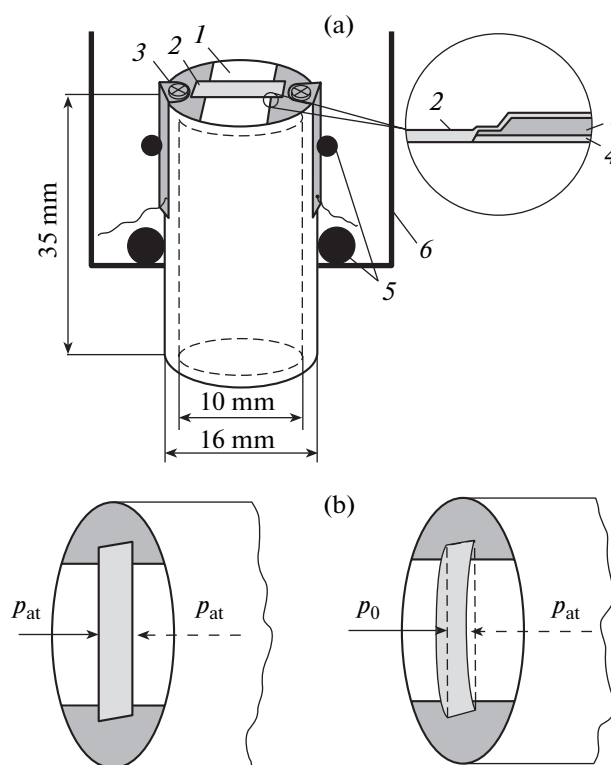


Fig. 1. (a) Schematic of the pressure sensor and (b) principle of its operation: (1) PTFE membrane, (2) sensitive element, (3) copper contact pads, (4) Cr film, (5) rubber seals, and (6) vacuum chamber wall. p_0 and p_{at} are the residual pressure and atmospheric pressure, respectively.

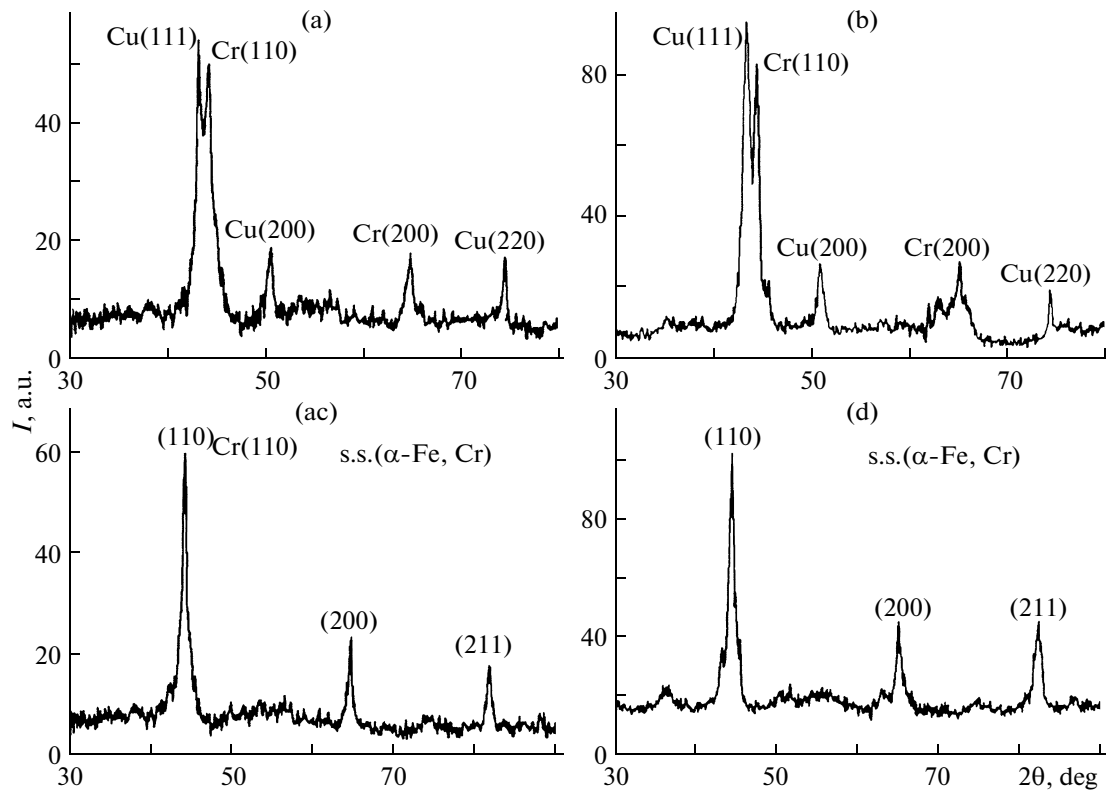


Fig. 2. X-ray diffraction patterns taken of the film (a, c) [Cu(30)/Cr(30)]₂/substrate and (b, d) [Fe(10)/Cr(10)]₂/substrate systems in the (a, b) as-grown and (c, d) annealed (630 K) states (the numbers in parentheses are thickness in nanometers).

chromel–alumel thermocouple and a UT-70B voltmeter). The thickness of the element was measured with a quartz resonator accurate to 10% and with an MII-4 interferometer. The resistance was measured using an ARRA-109 digital voltmeter accurate to 0.06%.

The phase composition was determined by the X-ray diffraction method with an X'Pert PRO instrument, and diffusion processes were studied by secondary ion mass spectrometry. The surface and interface roughnesses of the film pressure-sensitive elements were determined by the method of low-angle X-ray diffraction [12] using the X-Pert Reflectivity program package.

RESULTS AND DISCUSSION

The sensor exploits the tensorial properties of the sensitive element (Fig. 1b): when the pressure in the working volume changes relative to the ambient (atmospheric) pressure, the elements deform, generating mechanical stresses, which change the resistance. Thus, materials used to fabricate pressure-sensitive elements must have a high gauge factor and stable characteristics in the working ranges of pressure and temperature.

It seems that the pressure-sensitive element is the easiest to fabricate on the basis of a Cr film, since it offers good adhesion to the membrane material. It was

shown however [13], that the gauge factor of Cr elements reaches 40 only in the plastic strain range ($\epsilon_1 = 10\%$); therefore, chromium cannot be used as a material for the sensor, since it can stably operate only in the elastic strain range.

A possible way of increasing the gauge factor is the transition from a single-layer to a multilayer system, since an additional charge carrier scattering mechanism arises in the latter: scattering at interfaces. We prepared pressure-sensitive layers based on two-layer and multilayer Cu/Cr and Fe/Cr film systems. The lower Cr layer having a high adhesion to the membrane was covered by the upper Cu or Fe layer.

The film structures were selected from the following reasoning. According to related phase diagrams [14] and the data for phase states (Fig. 2) and diffusion (Fig. 3) in the systems we are interested in, the layers of the Cu/Cr system keep their inherent properties and the phase composition of the system as a whole is stable (fcc Cu and bcc Cr, lattice parameters $\bar{a} = 0.360\text{--}0.361$ nm for Cu and $\bar{a} = 0.288\text{--}0.289$ nm for Cr at relatively high temperatures), while the Fe/Cr system produces a Fe–Cr solid solution even at the condensation stage, which persists after annealing at 630 K and has a bcc lattice with lattice parameter $\bar{a} = 0.289 \pm 0.001$ nm.

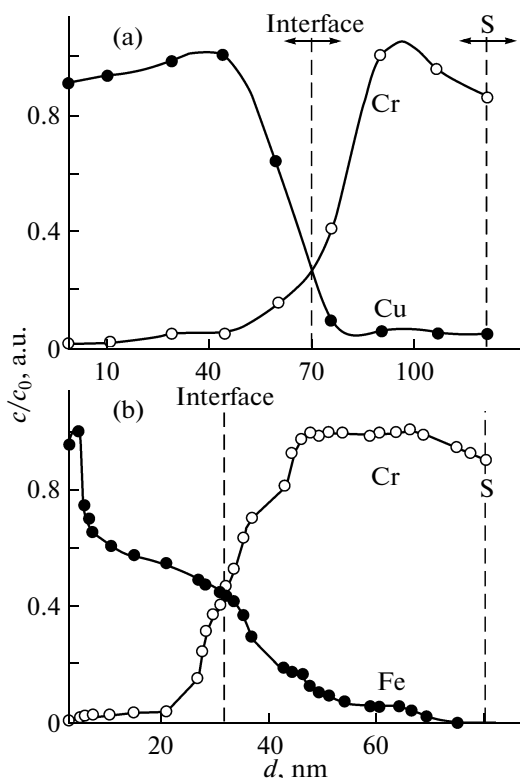


Fig. 3. Diffusion profiles of the relative concentration for the film (a) Cu(80)/Cr(40)/substrate and (b) Fe(40)/Cr(40)/substrate systems in the as-grown states. The data for the Fe(40)/Cr(40)/substrate system are taken from [15].

In addition, it was found [6] that coefficient γ_1 for the Cu/Cr system increases from $\gamma_1 = 2-4$ (the total thickness of the sample is $d = 30$ nm) to $\gamma_1 = 22-28$ ($d = 60$ nm). This takes place both at a constant thickness of the Cu layer and when the Cr layer gets thicker. For the Fe/Cr system, γ_1 is typically equal to 15–20 [17]. Thus, Cu/Cr and Fe/Cr systems are promising for sensitive elements of both strain gauges and pressure sensors.

Table

| [Cr(30)/Cu(30)] ₂ /SiO ₂ | | | [Fe(6)/Cr(7)] ₃ /Si | | |
|--|---------------|---------------|--------------------------------|---------------|---------------|
| Layer | <i>d</i> , nm | σ , nm | Layer | <i>d</i> , nm | σ , nm |
| Substrate SiO ₂ | — | 1.10 | Substrate Si | — | 1.79 |
| Cu | 30.2 | 1.07 | Cr | 10.7 | 0.94 |
| Cr | 30.0 | 3.83 | Fe | 9.9 | 0.35 |
| Cu | 30.2 | 1.03 | Cr | 10.2 | 1.18 |
| Cr | 31.2 | 1.90 | Fe | 10.1 | 0.44 |

Figure 4 shows typical performance characteristics of the pressure sensor. The curves are seen to have two distinct portions, one of which is nearly linear. As Δp grows, so does relative variation of resistance $\Delta R/R$, which is a graphic manifestation of the tensoresistive effect. In the second portion, the resistance varies with pressure nonmonotonically. The linear portion corresponds to pressures from 20 to 40 Pa in the vacuum chamber; therefore, the sensor can be used for measuring forevacuum pressure in vacuum setups. The reason for the drastic rise in the resistance in the second portion is a change in the rate of working chamber evacuation when the pumping facility is adjusted to a high vacuum.

From the performance characteristics, we calculated pressure coefficient of resistance $\beta_p = R^{-1}dR/dp$. In the Cu/Cr system, β varies between 1.50×10^{-3} and $0.12 \times 10^{-3} \text{ Pa}^{-1}$ for thicknesses $d = 50-120$ nm; in the Fe/Cr system, between 0.50×10^{-3} and $0.35 \times 10^{-3} \text{ Pa}^{-1}$ for $d = 40-80$ nm.

The presented performance characteristics do not allow us to directly measure the pressure during the operation of the device; however, bearing in mind the definition of the pressure coefficient of resistance and carrying out simple mathematical transformations, one can obtain a dependence of the resistance of the sensitive element on the pressure in the vacuum chamber:

$R(p) = R(p_0)e^{\beta_p p}$, where $R(p_0)$ is the resistance at atmospheric pressure. Atmospheric pressure p_a was measured with a standard barometer.

The stable operation of any sensor (including a pressure sensor) in which a multilayer film system serves as a sensitive element depends on the quality of interfaces, which was analyzed with regard to recommendations given in [18].

Figure 5 exemplifies X-ray reflectometry data for the [Cr(30)/Cu(30)]₂/SiO₂ and [Fe(10)/Cr(10)]₂/Si systems, and the table lists the calculated thicknesses of the layers and roughnesses σ of the interfaces.

As follows from Fig. 5a, interface roughness σ for the Cu/Cr system varies between 1.07 and 1.53 nm at room temperature. These values are in agreement with the results obtained in [18, 19] for Fe/Nb/Fe [19] and A/Co [18] systems with restricted mutual solubility ($\sigma = 0.9-1.2$ nm at $T_a \leq 270$ K and 1.5–4.5 nm at $T_a = 270-530$ K) and support the conclusion that the interface roughness in the systems studied is fairly high. This may deteriorate the stability of sensitive elements on their basis. The interface roughness obtained for the Fe/Cr system ($\sigma = 0.35-1.18$ nm, Fig. 5b) agrees with the results obtained in [20] for the Fe/Cr system ($\sigma \cong 0.2$ nm) and Cr/Fe system ($\sigma \cong 0.8$ nm) and also with the results obtained in [19] for the Fe/V/Fe system ($\sigma \cong 0.3$ nm). Thus, the interface roughness in the Fe/Cr system, in which a Fe–Cr solid solution forms throughout its volume, may be lower than in the Cu/Cr system, in which the layers keep their specific properties.

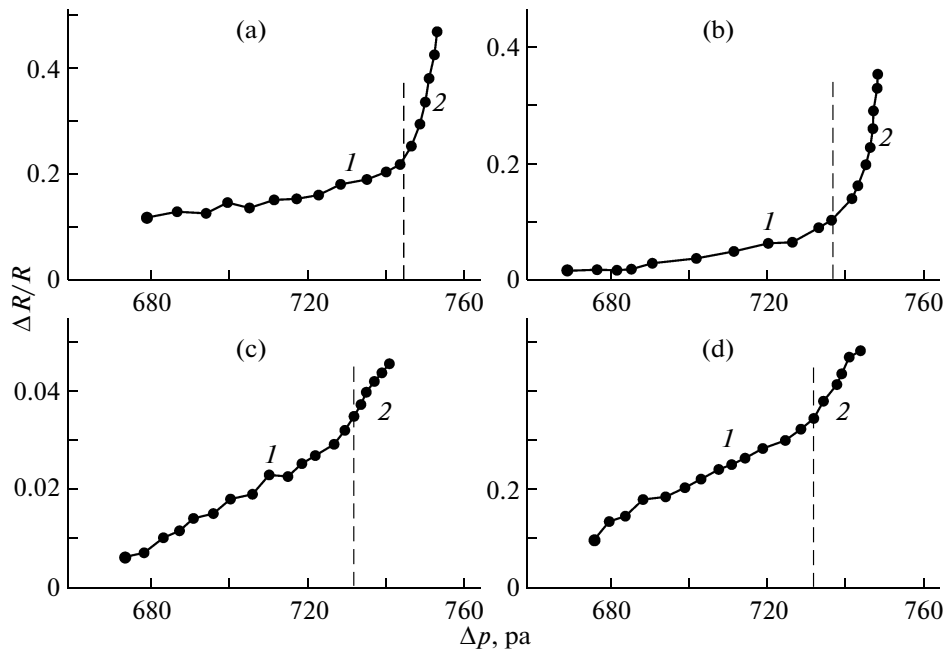


Fig. 4. Performance characteristics of pressure sensors based on (a) $[\text{Cu}(20)/\text{Cr}(20)]_2/\text{substrate}$, (b) $[\text{Cu}(10)/\text{Cr}(15)]_2/\text{substrate}$, (c) $[\text{Fe}(15)/\text{Cr}(15)]_2/\text{substrate}$, and (d) $[\text{Fe}(10)/\text{Cr}(10)]_2/\text{substrate}$ systems. $\Delta p = p_{\text{at}} - p_0$.

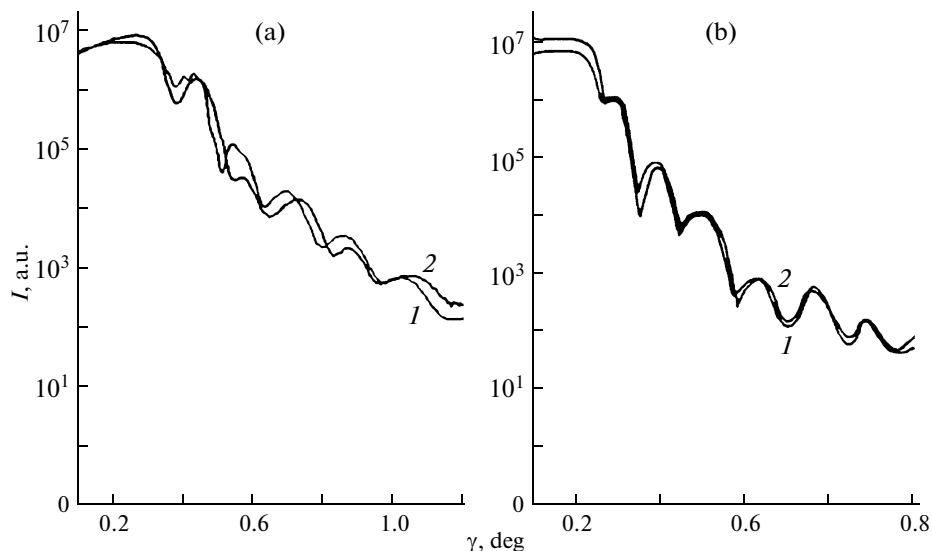


Fig. 5. X-ray reflectometry data curves for the film (a) $[\text{Cr}(20)/\text{Cu}(20)]_2/\text{SiO}_2$ and (b) $[\text{Fe}(10)/\text{Cr}(10)]_2/\text{Si}$ systems (γ is the angle). (1) Experiment; 2, numerical simulation.

CONCLUSIONS

Our investigations suggest that Cu/Cr and Fe/Cr film systems can be used as a sensitive element in pressure sensors. They have a stable phase composition (namely, fcc Cu + bcc Cr and Fe–Cr solid solution, respectively) in a wide temperature range.

Analysis of diffusion processes and interface roughness shows that the interface in the Fe/Cr system is smoother ($\sigma = 0.35\text{--}1.18$ nm).

REFERENCES

1. V. A. Kagadei, E. V. Nefedtsev, V. I. Proskurovskii, et al., *Pis'ma Zh. Tekh. Fiz.* **29** (21), 40 (2003) [*Tech. Phys. Lett.* **29**, 897 (2003)].
2. C. P. O. Treutler, *Sens. Actuators A* **91**, 2 (2001).
3. D. E. Kirichenko, A. B. Pavolotskii, I. G. Prokhorova, et al., *Zh. Tekh. Fiz.* **69** (7), 112 (1999) [*Tech. Phys.* **44**, 839 (1999)].
4. D. Belavic, M. Hrovat, and M. Pavlin, *J. Eur. Ceram. Soc.* **21**, 1989 (2001).

5. G.-S. Chugn, *Sens. Actuators A* **135**, 355 (2007).
6. A. Amor Ben, T. Budde, and H. H. Gatzert, *Sens. Actuators A* **126**, 41 (2006).
7. Kai Wah Yeung and Chung Wo Ong, *Sens. Actuators A* **137**, 1 (2007).
8. G. Schuler, M. Schmitt, D. Goettel, et al., *Sens. Actuators A* **126**, 287 (2006).
9. S.-P. Chang and M. G. Allen, *Sens. Actuators A* **116**, 195 (2004).
10. A. V. Shirinov and W. K. Schomburg, *Sens. Actuators A* **142**, 48 (2008).
11. Teng Lin, Yang Bang Chao, Du Xiao Song, et al., *Sens. Actuators A* **118**, 222 (2005).
12. V. Holly, V. Pietsh, and T. Baumbach, *High-Resolution X-Ray Scattering from Thin Films and Multilayers* (HPC, Heidenberg, 1999).
13. E. O. Zabala and I. Yu. Protsenko, *Ukr. J. Phys.* **50**, 727 (2005).
14. *Phase Diagrams of Binary Metallic Systems: A Handbook*, Ed. by N. P. Lyakishev (Mashinostroenie, Moscow, 1996) [in Russian].
15. V. V. Bibyk, L. V. Odnodvoretz, and I. A. Shpetnyi, *Vestn. Sumsk. Univ., Ser.: Fiz., Mat., Mekh.*, No. 9 (93), 91 (2006).
16. D. V. Velikodnyi, T. Grichanovskaya, L. V. Odnodvoretz, et al., *Vestn. Sumsk. Univ., Ser.: Fiz., Mat., Mekh.*, No. 1, 5 (2007).
17. D. V. Velikodnyi, S. I. Protsenko, and I. E. Protsenko, *Fiz. Inzheneriya Poverkhnosti* **6**, 37 (2008).
18. S. Kundu, *Nucl. Instrum. Methods Phys. Res. B* **242**, 542 (2006).
19. I. A. Garifullin, N. N. Garif'yanov, and R. I. Salikhov, *Izv. Ross. Akad. Nauk, Ser. Fiz.* **71**, 280 (2007).
20. M. Marszalek, V. Tokman, S. Protsenko, et al., *Vacuum*, No. 10, 1051 (2008).

SPELL OK